JOURNAL OF MATERIALS SCIENCE 31 (1996) 2447–2455

Processing and microstructural development of reaction-bonded sintering of a Si_3N_4/intermetallic composite

F. MARINO
Dipartimento di Scienza dei Materiali e Ingegneria Chimica, Politecnico di Torino, Corso Duca degli Abruzzi 24-10129 Torino, Italy

B. R. ZHANG*
Department of Inorganic Materials, Shandong Institute of Light Industry, 250100 Jinan, People's Republic of China

B. FORNARI
Alenia Spazio spa, corso Marche 41, 10146 Torino, Italy

This paper focuses on the reaction-bonded sintering of a Si_3N_4/intermetallic composite. The preparation process and the microstructural characterization of this composite with different initial contents of Ni_3Al have been investigated. The effects of Ni_3Al addition on the nitridation of silicon and the $\alpha \rightarrow \beta$ phase transformation of Si_3N_4 formed, as well as the densification of the composite, also have been discussed. The addition of Ni_3Al particles accelerates the nitriding rate of silicon and results in the formation of β-Si_3N_4 phase at low temperature due to the reaction occurring between silicon and Ni_3Al. Consequently, a completely nitrided and denser composite, compared with reaction-bonded sintered Si_3N_4, was obtained at low temperature. For comparison, pure silicon simultaneously processed was also investigated.

1. Introduction

Silicon nitride (Si_3N_4) based ceramics are presently being considered for heat engine applications because of their high-temperature strength, oxidation resistance, thermal stability, chemical stability and thermal shock resistance. Much research has been concerned with improving their fracture toughness by the addition of silicon carbide (SiC) whiskers [1, 2] or metallic fibres [3] and by the formation of *in situ* elongated, fibrous β-Si_3N_4 [4]. In the composite approach, the incorporation of whiskers or fibres into the Si_3N_4 matrix allows dissipative mechanisms [5], such as crack bridging and crack deflection, to increase the work of fracture. However, the preparation of whisker-reinforced composites remains problematic due to the difficulties in processing and due to the high cost of the whiskers. In self-reinforced mechanisms, due to their fibrous morphology, the β-grains can play a role similar to that of SiC whiskers in the composite, but, this process is based on the addition of various sintering aids such as MgO, Y_2O_3, Al_2O_3, Sc_2O_3, Li_2O, etc. [6, 7]. The type and the amount of sintering additives, required to form a suitable liquid [8, 9], determine not only the densification rate and the processing temperature, but also the microstructure such as grain-boundary phase characteristics, which control the high-temperature properties. Usually, these sintering aids lead to the degradation of the high-temperature properties [10].

The present work focuses on one new type of Si_3N_4-based material: Si_3N_4/intermetallic composite. Intermetallic compounds have emerged as the next generation of high-temperature, oxidation-resistant materials [11]. Compared with the commonly used additives for Si_3N_4, the intermetallic compounds, e.g. Ni_3Al, have many interesting properties, such as high elastic modulus, high yield strength, high rupture strength and especially their anomalous thermal hardening behaviour, in which strength increases with temperature up to approximately 800 °C [12]. In order to avoid the intrinsic brittleness of pure Ni_3Al, rapidly solidified nickel aluminide powders with improved properties, labelled as 465# in the literature [13], which contain B (0.10 at %) and Cr (8 at %) have been used in the present work.

Good high-temperature mechanical properties might be expected for this composite because at elevated temperature most intermetallic compounds would act as ductile phases. Having considered the difficulties in sintering

* To whom correspondence should be addressed. Present address: Dipartimento di Scienza dei Materiali e Ingegneria Chimica, Politecnico di Torino, Corso Duca degli Abruzzi 24, 10129 Torino, Italy.

0022–2461

Si_3N_4 and the difference in melting points between Si_3N_4 and Ni_3Al, a method of preparation of this composite followed the reaction-bonded sintering method, taking inexpensive silicon powder mixed with 465# Ni_3Al powders as raw material. In a previous work [14] the chemical aspects of reaction-bonded sintering of Si_3N_4/Ni_3Al system was investigated, while this paper mainly focuses on the preparation process and on the microstructural development of this composite containing different initial amounts of Ni_3Al. The effects of Ni_3Al addition on the nitriding rate of silicon, the $\alpha \rightarrow \beta$ Si_3N_4 phase transformation in presence of Ni_3Al and the densification of the composite have also been discussed.

2. Experimental procedure

Commercial silicon powders (99.5 %, 325 mesh, Johnson Matthey GmbH) were ball milled to a particle size less than 1 μm and carefully mixed with 0, 1, 5 and 10 vol % Ni_3Al particles (465#, < 50 μm, kindly supplied by R. N. Wright and J. R. Knibloe, INEL Lab. [13]) with respect to the final Si_3N_4. The powder mixtures were cold-pressed using a uniaxial stainless-steel die. The pressure of formation used was 80–100 MPa, producing green compacts with a density of about 60 % of the theoretical value. Some samples were shaped by the CIP (cold-isostatic pressed) method, producing a bulk density similar to that of single-action pressed. The pressed compacts were presintered at 900–1100 °C for 2–10 h, whereas reaction conditions varied between 1200 and 1250 °C for 5–80 h. All presintering and reaction-sintering were carried out in a tube furnace and the nitriding gas was a mixture of purified $N_2 + 5$ % H_2 ($N_2 > 99.999$ %, $H_2 > 99.9995$ %, respectively) at atmospheric pressure. These samples were laid on a powder bed of Si_3N_4 which was on an alumina support. Pure silicon compacts were either nitrided under the same conditions or continuously nitrided at 1450 °C for 2–10 h for reference material samples. The samples, as a function of their Ni_3Al content, have been named SN for silicon nitrided only, and SN/NA 1, SN/NA 5 and SN/NA 10 for those containing 1, 5 and 10 vol % Ni_3Al, respectively.

Densities of samples were determined before and after nitriding by weight and volume measurements and by Archimedes principle. The extent of nitridation was determined by the ratio between the weight of the sample under nitridation and its theoretical weight assuming that all the silicon was converted into Si_3N_4. The nitride phases were investigated by X-ray diffraction (XRD) analyses, using CuK_α radiation monochromated in the diffracted beam, on the core of the samples. The microstructure was characterized by scanning electron microscopy (SEM) and analysed by energy dispersion X-ray spectroscopy (EDXS).

3. Results and discussion

3.1. Nitridation of the Si + Ni_3Al system

The X-ray diffraction patterns of the nitrided samples prepared at 1250 °C for 20 h are shown in Fig. 1, which shows firstly the absence of the Ni_3Al characteristic reflections and secondly the formation of much larger quantities of either α- or β-Si_3N_4 phases in Ni_3Al-added system than in the pure silicon sample.

The microstructure of the nitrided sample without Ni_3Al (SN) is composed only of silicon and α-silicon nitride (α-Si_3N_4). With the addition of Ni_3Al, other phases than silicon and α-Si_3N_4, especially β-silicon nitride (β-Si_3N_4), were found in the nitrided samples. In Fig. 1, it is shown that, for the samples containing different Ni_3Al contents and nitrided under the same conditions, the amount of β-Si_3N_4 phase increases with increasing Ni_3Al content. This conclusion was confirmed by the X-ray analyses on the samples nitrided at 1250 °C for 5, 10, 15 as well as for 40, 60 and 80 h.

Figs 2 and 3 show, respectively, the X-ray diffraction patterns of the nitrided samples sintered at 1250 °C for 40 and 80 h.

For the nitrided samples, containing the same quantity of Ni_3Al sintered for different times, the α/β ratio decreases with increasing nitriding time. Certainly, the nitrided samples prepared at 1250 °C contain more β-Si_3N_4 than those prepared at 1200 °C under the same conditions. Furthermore, in the sample containing 10 vol % Ni_3Al nitrided at 1250 °C for more than 40 h, almost all the α-Si_3N_4 phase is transformed into β-Si_3N_4. In contrast, no detectable amount of β-Si_3N_4 phase was found in SN samples nitrided under the same conditions, not even in those nitrided at 1250 °C for 80 h. Similarly, as mentioned above, in the nitrided samples, the amount of free silicon decreases with increasing Ni_3Al addition. Only a very little amount of Si phase was detected in SN/NA 10 nitrided at 1250 °C for 20 h and in SN/NA 5 nitrided at the same temperature for 40 h. However, a large quantity of Si was found in SN nitrided at 1250 °C for 80 h, as shown in Fig. 3. On the other hand, in the SN sample, nitrided first at 1250 °C for only 5 h and then at 1450 °C for 2 h, only traces of silicon were detected, as indicated in Fig. 4. This demonstrates the strong influence of nitriding temperature on the conversion of Si in the SN samples.

Usually, the nitridation or reaction-bonding process is carried out under a nitrogen atmosphere at temperatures ranging up to 1420 °C for several days ($\leqslant 1420$ °C, $\geqslant 72$ h) [15]. From the results of the present work, the SN sample was partially nitrided (about 82 % calculated from the weight gain) at 1250 °C up to 80 h, resulting mainly in the α-Si_3N_4 phase, while almost all the silicon phase was converted at 1250 °C for 20 h in SN/NA 10 and for 40 h in SN/NA 5. Besides, unlike the microstructure of the nitrided sample of pure silicon, the addition of Ni_3Al increased the β-Si_3N_4 phase. This means that the increasing nitriding rate in the Ni_3Al-added system is partially attributed to the formation of β-Si_3N_4 phase at low temperature. Comparing the X-ray diffraction patterns of SN/NA 1 and SN, in all the sintering treatments, SN/NA 1 shows the rise of β-Si_3N_4 and a larger quantity of α-Si_3N_4. A very small peak of Si phase in SN/NA 1 nitrided at 1250 °C for 80 h forms a striking contrast with the intense occurrence of Si in SN sample simultaneously processed (Fig. 3). Thus it can

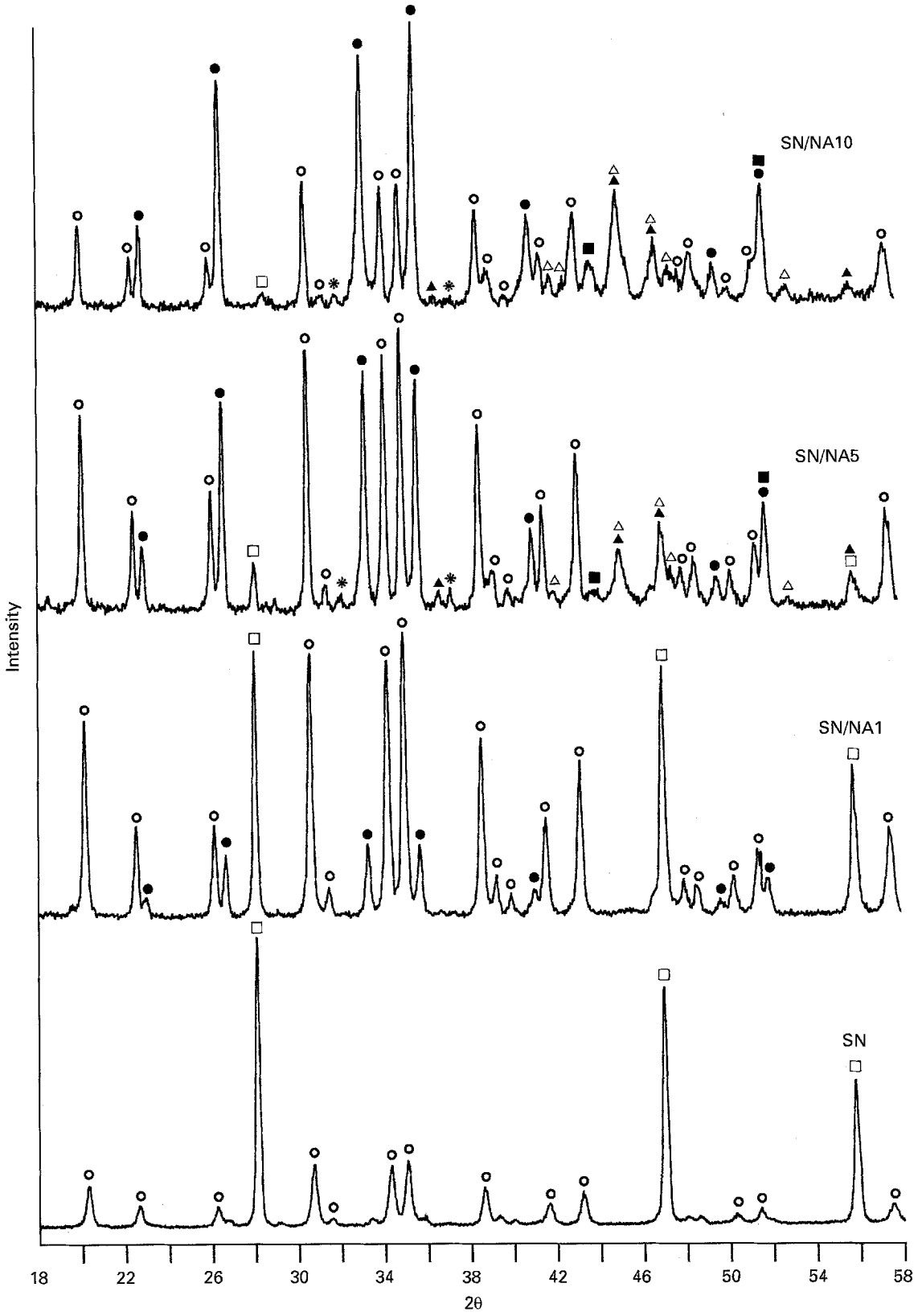

Figure 1 X-ray diffraction patterns of the samples nitrided at 1250 °C for 20 h: (○) α-Si_3N_4, (●) β-Si_3N_4, (□) Si, (▲) NiSi, (△) $Ni_{31}Si_{12}$, (■) Cr_3Si, (∗) AlN.

be said that the addition of Ni_3Al has accelerated the formation of α-Si_3N_4 as well.

According to the formation mechanisms of the different Si_3N_4 phases, the α-phase is preferably formed at temperatures below the melting point of silicon through a gas-phase reaction, while the β-modification may be formed by a solid–gas reaction between silicon and nitrogen and through diffusion of nitrogen in solid silicon nitride or in the presence of a liquid phase [15].

The increase of β-phase, due to the nitridation of the Si sample at a temperature above the silicon melting point (X-ray diffraction pattern is shown in Fig. 4), can be used to explain that the β-phase formation is

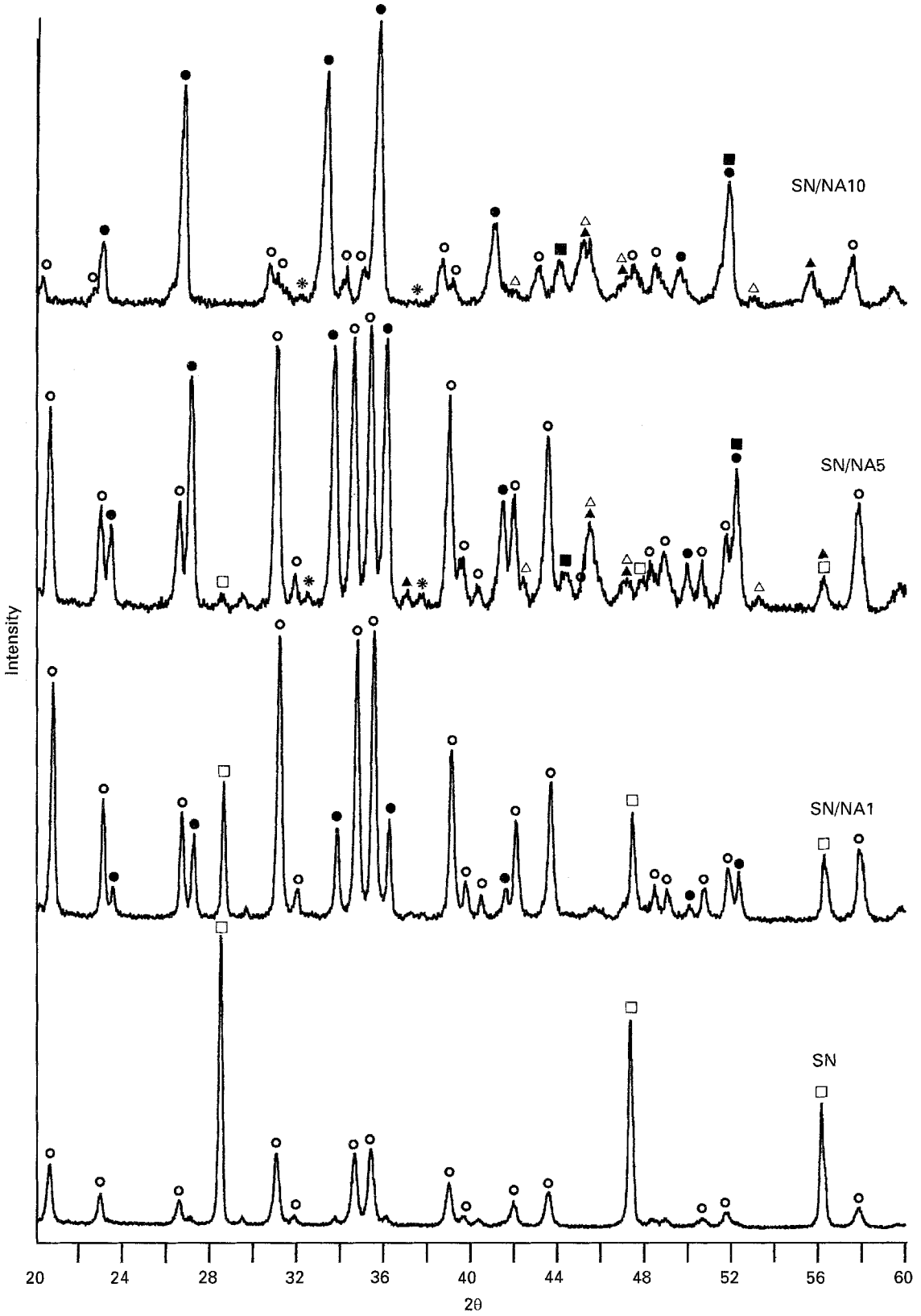

Figure 2 X-ray diffraction patterns of the samples nitrided at 1250 °C for 40 h: (○) α-Si_3N_4, (●) β-Si_3N_4, (□) Si, (▲) NiSi, (△) $Ni_{31}Si_{12}$, (■) Cr_3Si, (*) AlN.

associated with the existence of a liquid phase. As for the high proportion of β-phase formed in the Ni_3Al-added system at a low temperature such as 1250 °C, it has been hypothesized that this is due to a liquid phase resulting from the reaction of Ni_3Al with Si and N_2. In a previous paper of ours [14], in order to investigate the liquidus temperature of the $Si/Ni_3Al/N_2$ system, a DTA + TG experiment was performed on a mixture of Si + 10 vol % Ni_3Al in a $N_2 + 5\%H_2$ atmosphere. The formation of a liquidus phase occurred at about 1100 °C. Several works [16–18] have illustrated that the phase transformation is always accompanied by the solution of α-grains and the reprecipitation of β-modified phase.

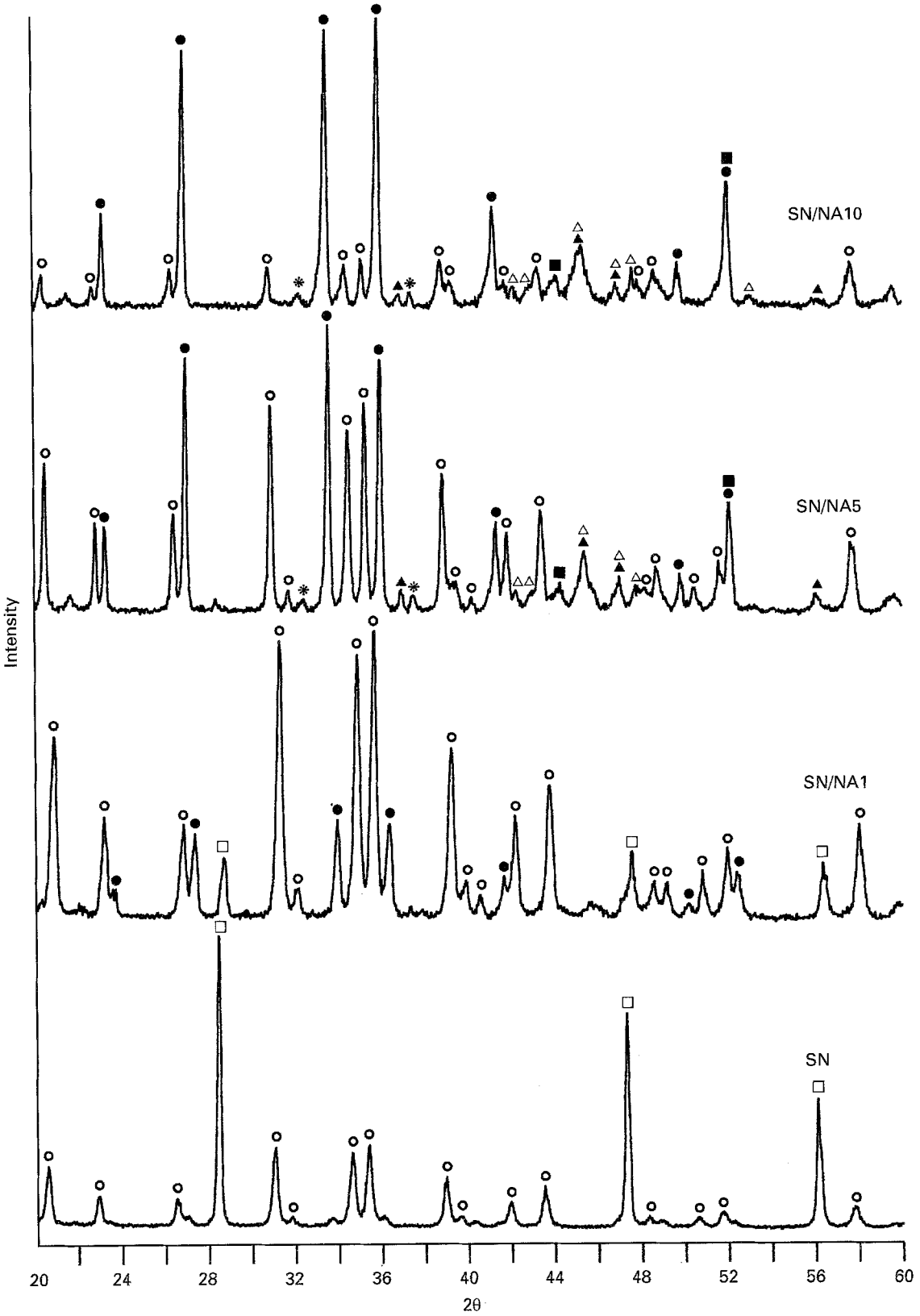

Figure 3 X-ray diffraction patterns of the samples nitrided at 1250 °C for 80 h: (○) α-Si_3N_4, (●) β-Si_3N_4, (□) Si, (▲) NiSi, (△) $Ni_{31}Si_{12}$, (■) Cr_3Si, (*) AlN.

For example, the work [16] in which 10 wt % Fe was added to investigate its effect on nitridation of silicon has demonstrated that the acceleration of the nitridation by Fe was due to the formation of a low melting point compound $SiFe_x$.

According to the X-ray analyses, the main reaction products between Ni_3Al and Si correspond to the chemical formulas NiSi, $Ni_{31}Si_{12}$ as well as Cr_3Si. It is difficult to identify all the formulas accurately, but through X-ray mapping [14] it has been confirmed that they are silicides of nickel and chromium. Moreover, the work [19] has indicated that increasing the chromium content of the nickel-based alloys tends to increase the interaction between the alloy and silicon

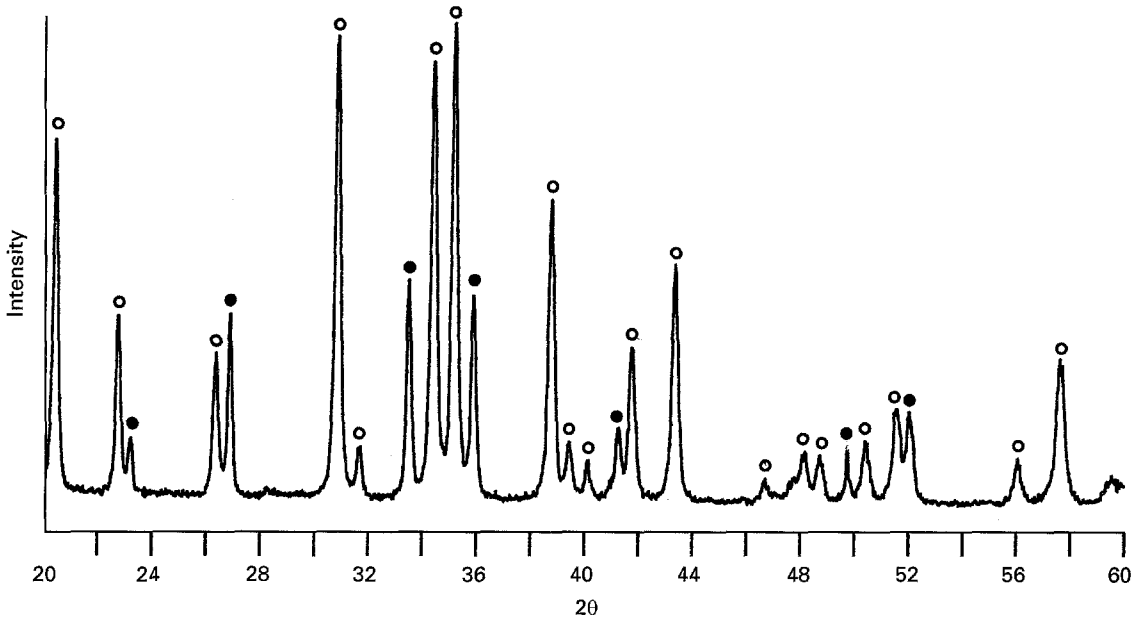

Figure 4 X-ray diffraction patterns of the Si sample nitrided at 1250 °C for 5 h and at 1450 °C for 2 h: (○) α-Si_3N_4, (●) β-Si_3N_4.

nitride. However, for high-temperature applications, according to [20], the interface formed by Cr–Si_3N_4 reactions would be preferable to that formed by Ni–Si_3N_4 reactions, because of the higher eutectic temperatures of the Cr–Si system (1345 °C versus 964 °C). For the Cr–Ni–Si system, a minimum ternary eutectic temperature of 1077 °C is known from the same article [20]. In any case, it can be inferred that the liquid phase is present at the nitridation temperature of 1250 °C and, consequently, the β-Si_3N_4 formation and the $\alpha \rightarrow \beta$ phase transformation were enhanced. Besides, the products of the reaction of Ni_3Al with N_2 were also examined by X-ray diffraction, and energy dispersive X-ray spectroscopy (EDXS) mapping [14] confirmed the presence of AlN. In fact, the formation of AlN was also found, by the reaction of aluminium in a Ni-base alloy with silicon nitride [21], and was also seen in another work [16] which investigated the effect of Al additions on nitridation of silicon.

On the other hand, the accelerating effect of Ni_3Al on the nitridation of Si may be explained by considering the fact that nitrogen can easily diffuse and, consequently, easily react with silicon since Ni_3Al particles are a few orders of magnitude larger than the submicrometre silicon powders. This can be supported by the phenomenon of homogeneous nitriding either at the surface or inside samples with added Ni_3Al; this fact has been confirmed not only by X-ray diffraction but also by observation of colour. On the contrary, in the SN sample, the surface was nitrided more rapidly; for this reason nitrogen permeation becomes more difficult and leads to large unreacted silicon grains.

3.2. Nitriding rate and densification

For pure silicon, the nitrided fraction can be determined by the ratio between the weight of the nitrided sample and the initial sample weight multiplied by 1.6649, according to the stoichiometry of the reaction. For samples containing Ni_3Al powders, this method is incorrect because Ni_3Al completely reacts with N_2 and Si, and consequently a portion of Si, owing to the formation of Ni_xSi_y, is subtracted from the nitridation reaction. Therefore, the nitrided fraction is approximately calculated by the formula:

$$N_f = \frac{A - \mathrm{AlN} - \mathrm{Ni}_x\mathrm{Si}_y}{\mathrm{Si}_3\mathrm{N}_4}$$

where A is the weight of the sample at a certain step of the nitridation; AlN is the calculated weight of the aluminium nitride formed; Ni_xSi_y is the calculated weight of nickel silicides formed (hypothesizing 50 wt % NiSi + 50 wt % $Ni_{31}Si_{12}$); and Si_3N_4 is the calculated maximum weight of silicon nitride formed from free silicon (i.e. the silicon content minus the silicon involved in the formation of Ni_xSi_y). However, for SN/NA1 sample, 1 vol % Ni_3Al can be assumed to be a sintering-aid and the influence of the reaction between it and Si on the sample's weight change may be negligible. We have calculated the nitriding fraction of Si in SN/NA1 sample on the supposition that the weight of Ni_3Al would remain the same before and after the sintering. Table I shows the nitrided fraction of the samples containing different initial Ni_3Al, nitrided at 1250 °C for different times.

The results reported in Table I clearly demonstrate the accelerating effect of the addition of Ni_3Al on the nitridation of Si; this is also consistent with the XRD analyses. The nitriding fraction of each group of composites is higher than that of the SN sample. As for composite samples containing different initial contents of Ni_3Al, with nitriding times shorter than 20 h, the nitrided fraction in SN/NA1 is higher than in SN/NA5 and SN/NA10. But after 20 h nitriding, the nitriding fraction increases with the initial content of

TABLE I Nitrided fraction of the samples containing different initial content of Ni_3Al

Sample name	Initial Ni_3Al content (vol %)	Nitrided fraction (%) for various times (h) at 1250 °C						
		5	10	15	20	40	60	80
SN	0	76.81	77.97	78.61	78.98	80.30	81.20	82.02
SN/NA1	1	84.96	87.19	88.54	89.53	91.85	92.85	93.42
SN/NA5	5	81.68	85.68	88.36	90.29	93.10	93.41	94.69
SN/NA10	10	81.26	85.78	88.70	90.52	93.44	94.21	—

TABLE II Densities of some samples

Samples	Process (°C × h)	Density (g cm^{-3})	Relative density (%)	Theoretical density (g cm^{-3})
SN	1250 × 80	2.36	74.68	3.16[a]
	1250 × 50 + 1450 × 10	2.70	85.44	
SN/NA1	1250 × 80	2.86	89.28	3.2034[b]

[a]The density of α-Si_3N_4.
[b]The densities calculated according to the sample compositions, on the supposition that Ni_3Al does not react with Si.

Ni_3Al. This is related to the quantities of the liquid phase. Furthermore, it can be observed from Table I, for SN, that the nitriding rate is maximum at the initial stage and decreases with increasing nitriding time, reaching only about 82% at 80 h. On the other hand, as shown in Fig. 4, only traces of silicon were found in the sample nitrided at 1250 °C for 5 h and then at 1450 °C for 2 h; in this sample, according to the weight gain, the nitrided fraction reached about 90%. In another sample, nitrided at 1250 °C for 50 h and at 1450 °C for 10 h, about 96% silicon was nitrided. However, the relative density of this sample is only 85% (even when nitridation has reached 96%). Contrarily, in the SN/NA1 sample nitrided at the same low temperature, 1250 °C for 80 h, and although Si phase is still detected, the nitrided fraction reached 93.42% and the relative density 89.28%, compared with 82.02% and 74.68% for SN.

Table II shows the densities of some samples measured according to Archimedes principle, in which the results for SN/NA5 and SN/NA10 have not been included because of the difficulty in deciding their theoretical densities.

On the other hand, for the SN/NA10 sample nitrided for 80 h, a weight loss of about 0.57 %, compared with that of a similar sample nitrided for 60 h was observed. This may be due to the evaporation of intermetallics formed during the process. In fact, weight loss should accompany the whole nitriding process, as the formation temperatures of the liquid phase are lower than the sintering temperature. The weight loss is evident only after 60 h as previous to this it was counterbalanced by the weight increase due to the nitridation process.

In addition, from the comparison of samples pressed by a single-action die and by CIP, it can be said that the shaping method has little effect on nitridation and densification in the reaction-bonded sintering process. From dimensional measurement, it has been observed that no shrinkage occurred for the reaction-bonded sintering of this composite, which is also one of the outstanding advantages of RBSN.

3.3. Microstructure comparison

As previously discussed, the microstructure of reaction-bonded sintered Si_3N_4/Ni_3Al composite is very different from that of RBSN. Fig. 5 shows the SEM micrograph of the fracture surface of the SN sample nitrided at 1250 °C for 50 h and at 1450 °C for 10 h. The microstructure consists mainly of α- and β-phases, unreacted Si as well as macro- and micropores. This sample has a residual porosity of about 15%. The micropores are distributed in the same region as the fine α-needles. In contrast, in the vicinity of macropores, rod-like β-phase is formed.

In the composite, except for grains of α-Si_3N_4, α-whiskers are formed either at the sample surface or close to the macropores. Fig. 6 shows the fracture surface of a SN/NA10 sample nitrided at 1250 °C for

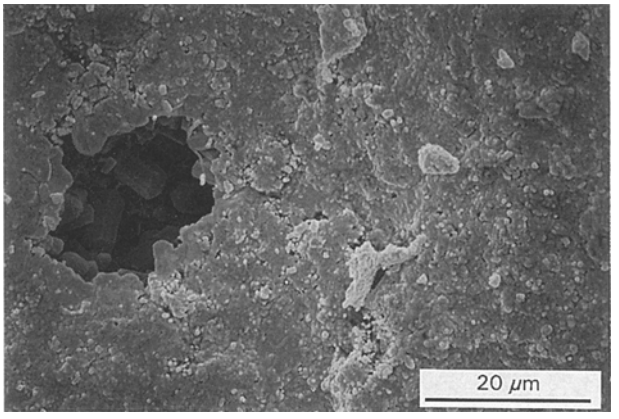

Figure 5 SEM micrograph showing the fracture surface of SN sample.

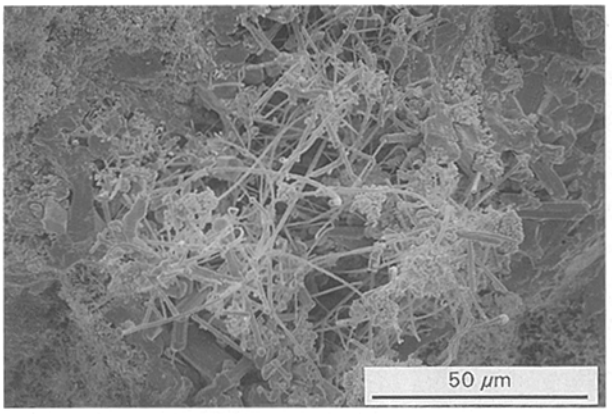

Figure 6 SEM micrograph showing α-whiskers forming near pores in the SN/NA10 sample nitrided for 40 h.

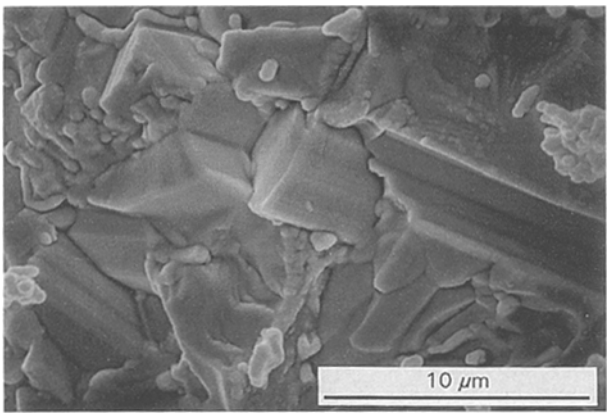

Figure 7 SEM micrograph showing β-phase forming in the region of the intermetallics.

40 h, in which α-whiskers are found in the more porous regions, which also favours the formation of rod-like β-phase. The formation of α-whiskers, as well as β-phase, is also probably due to the occurrence of a secondary liquid phase. The work [22] indicated that many of these whiskers originate from a spherical nucleus which frequently contains impurities such as iron, which can decrease the melting temperature of silicon by as much as 200 °C. Besides, the rod-like β-phase is formed not only near the pores, but also in the vicinity of the intermetallics because of the presence of a liquid-phase which partially dissolves α-grains and β-modified phase can reprecipitate easily. Fig. 7 shows the formation of β-phase in the region of intermetallics in SN/NA10 nitrided at 1250 °C for 40 h.

Fig. 8 shows the typical microstructure of SN/NA1 nitrided at 1250 °C for 80 h. It consists of a matrix, mainly α-Si_3N_4, an intermetallic zone (centre region in Fig. 8), consisting of nickel silicides and a transition region, i.e. around the intermetallics, which is usually porous. This is because the reaction products among Ni_3Al, N_2 and Si were formed in the very early stage (before the beginning of nitridation), which solidified on cooling from the nitridation temperature and formed the porous region around the intermetallic phases in the composite, just like it occurs in the formation of a typical porous structure of the crystal-

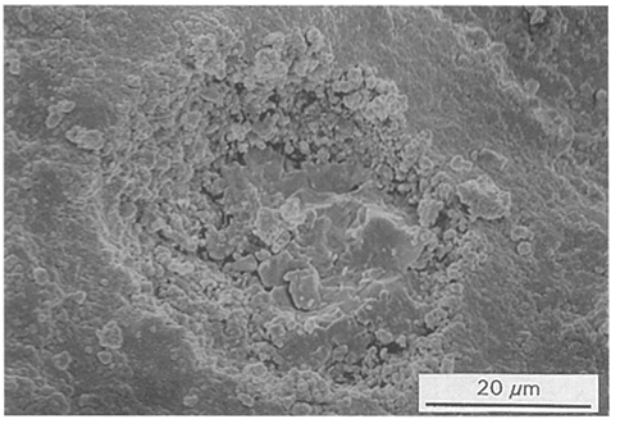

Figure 8 SEM micrograph showing the fracture surface of the SN/NA1 sample nitrided at 1250 °C for 80 h.

line secondary phase found in RBSN [23]. Furthermore, in this zone, the abnormal growth of β-grains may cause the porous structure.

4. Conclusions

The addition of Ni_3Al powders accelerates the nitridation of silicon and completely converts it at low temperature. The β/α Si_3N_4 ratio increases with the initial content of Ni_3Al not only because its particle size is up to 50 μm which makes nitrogen diffuse more easily but mainly due to the reaction of Ni_3Al with N_2 and Si.

The reaction of Ni_3Al with N_2 and Si occurs at a lower temperature than the nitridation of silicon, giving nickel and chromium silicides as reaction products with the corresponding chemical formulas NiSi, $Ni_{31}Si_{12}$ and Cr_3Si. The formation of low melting intermetallics originates from a liquid-phase and consequently enhances the densification of the composite.

The microstructure of the composites consists of α-, β-Si_3N_4, intermetallic phases and AlN, as well as pores. Except for α-Si_3N_4 grains, α-Si_3N_4 whiskers are also formed on the sample surface and close to the macropores. α-Si_3N_4 grains are found mainly in the matrices whereas β-modified phase is found in the vicinity of the intermetallic phases.

Acknowledgements

This work has been partially supported by Alenia Spazio spa Torino. We gratefully acknowledge Dr M. Ferraris and M. Raimondo, Department of Material Science and Chemical Engineering of Politecnico di Torino, for their help in the SEM observation.

References

1. G.C. WEI and P.F. BECHER, *Amer. Ceram. Soc. Bull.* **64** (1985) 298.
2. P.D. SHALEK, J.J. PETROVIC, G.H. HURLEY and F.D. GAC, *ibid.* **65** (1986) 351.
3. J.J. BRENNON, in "Special Ceramics 6", edited by P. Popper (British Ceramics Research Association, London, UK, 1975) p. 123.
4. A.J. PYZIK and D.R. BEAMAN, *J. Amer. Ceram. Soc.* **76** (1993) 2737.

5. F. ROSSIGNOL, P. GOURSAT, J.L. BESSON and P. LESPADE, *J. Eur. Ceram. Soc.* **13** (1994) 299.
6. T. EKSTROM and M. NYGREN, *J. Amer. Ceram. Soc.* **75** (1992) 259.
7. D. SUTTOR and G. S. FISCHMAN, *ibid.* **75** (1992) 1063.
8. K. H. JACK, in "Hayne-Palmour IV: Processing of Crystalline Ceramics", Vol. 11 (Material Science Research, Plenum, New York, 1978) p. 561.
9. F.F. LANGE, *Int. Metall. Rev.* **1** (1980) 1.
10. D.W. RICHERSON, *Amer. Ceram. Soc. Bull.* **52** (1973) 560.
11. A.I. TAUB and R.L. FLEISCHER, *Science* **243** (1989) 616.
12. R.M. GERMAN and A. BOSE, *Mater. Sci. and Eng.* **A107** (1989) 107.
13. R.N. WRIGHT and J.R. KNIBLOE, *Acta Metall. Mater.* **38** (1990) 1993.
14. B.R. ZHANG, S. GIALANELLA and F. MARINO, in 8th CIMTEC: International Congress on Modern Materials Technologies. Firenze, Italy, 29 June–4 July, 1994.
15. G. ZIEGLER, J. HEINRICH and G. WOTTING, *J. Mater. Sci.* **22** (1987) 3041.
16. M. MITOMO, *ibid.* **12** (1977) 273.
17. M. MITOMO and S. UENOSONO, *J. Amer. Ceram. Soc.* **75** (1992) 103.
18. J. HEINRICH, E. BACKER and M. BONMER, *ibid.* **71** (1988) C-238.
19. M.J. BENNETT and M.R. HOULTON, *J. Mater. Sci.* **14** (1979) 184.
20. M. MAKAMURA and S.D. PETEVES, *J. Amer. Ceram. Soc.* **73** (1990) 1221.
21. R.L. MEHAN, M.R. JACKSON, M.D. McCONNELL and N. LEWIS, *J. Mater. Sci.* **18** (1993) 508.
22. D.R. MESSIER and P. WONG, *J, Amer. Ceram. Soc.* **56** (1973) 480.
23. H. J. KLEEBE and G. ZIEGLER, *ibid.* **72** (1989) 2314.

Received 9 August 1994
and accepted 9 November 1995